



Identification of ALG3 as a potential prognostic biomarker in lung adenocarcinoma

Yinjiao Yuan^{a,c,1}, BaoCheng Xie^{b,1}, Dongbo Guo^{g,1}, Caixiang Liu^c,
Guanming Jiang^c, Guowei Lai^{d,e}, Yu Zhang^f, Xiarong Hu^d, Zhiming Wu^d,
Ruian Zheng^{c,**}, Linxuan Huang^{c,*}

^a The First School of Clinical Medicine, Southern Medical University, Guangzhou, 510510, China

^b Department of Pharmacy, Affiliated Dongguan Hospital, Southern Medical University, Dongguan, China

^c Department of Oncology, Dongguan Institute of Clinical Cancer Research, Dongguan Key Laboratory of Precision Diagnosis and Treatment for Tumors, The Tenth Affiliated Hospital of Southern Medical University (Dongguan people's hospital), Dongguan, 523059, China

^d Department of General Surgery, Affiliated Dongguan Hospital, Southern Medical University, Dongguan, China

^e General Hospital of Third Division, Xinjiang Production and Construction Corps, Tumushuker, China

^f The Sixth Affiliated Hospital of Sun Yat-sen University, Guangzhou, China

^g State Key Laboratory of Marine Resource Utilization in South China Sea, Key Laboratory of Biomedical Engineering of Hainan Province, School of Biomedical Engineering, Hainan University, China

ARTICLE INFO

Keywords:

Lung adenocarcinoma
ALG3
Prognostic biomarker
Immune infiltration

ABSTRACT

Background: The abnormal expression of Alpha-1,3-mannosyltransferase (ALG3) has been implicated in tumor promotion. However, the clinical significance of ALG3 in Lung Adenocarcinoma (LUAD) remains poorly understood. Therefore, we aimed to assess the prognostic value of ALG3 and its association with immune infiltrates in LUAD.

Methods: The transcriptional expression profiles of ALG3 were obtained from the Cancer Genome Atlas (TCGA), comparing lung adenocarcinoma tissue with normal tissues. To determine the prognostic significance of AGL3, Kaplan-Meier plotter, and Cox regression analysis were employed. Logistic regression was utilized to analyze the association between ALG3 expression and clinical characteristics. Additionally, a receiver operating characteristic (ROC) curve and a nomogram were constructed. To explore the underlying mechanisms, the Kyoto Encyclopedia of Genes and Genomes (KEGG) pathway enrichment analysis and gene set enrichment analysis (GSEA) was conducted. The relationship between AGL3A mRNA expression and immune infiltrates was investigated using the tumor immune estimation resource (TIMER) and tumor-immune system interaction database (TISIDB). Furthermore, an in vitro experiment was performed to assess the impact of ALG3 mRNA on lung cancer stemness abilities and examine key signaling pathway proteins.

Results: Our results revealed the ALG3 mRNA and protein expression in patients with LUAD was much higher than that in adjacent normal tissues. High expression of ALG3 was significantly associated with N stage (NO, HR = 1.98, P = 0.002), pathological stage (stage I, HR = 2.09, P = 0.003), and the number of pack years (<40, HR = 2.58, P = 0.001). Kaplan-Meier survival analysis showed that high expression of ALG3 was associated with poor overall survival (P <

* Corresponding author.

** Corresponding author.

E-mail addresses: 2857311978@qq.com (R. Zheng), huanglx6@mail2.sysu.edu.cn (L. Huang).

¹ Both authors contribute equally to this work.

<https://doi.org/10.1016/j.heliyon.2023.e18065>

Received 23 February 2023; Received in revised form 30 June 2023; Accepted 5 July 2023

Available online 8 July 2023

2405-8440/© 2023 The Authors. Published by Elsevier Ltd. This is an open access article under the CC BY-NC-ND license (<http://creativecommons.org/licenses/by-nc-nd/4.0/>).

0.001), disease-free survival ($P < 0.001$), and progression-free interval ($P = 0.007$). Through multivariate analysis, it was determined that elevated ALG3 expression independently impacted overall survival ($HR = 1.325$, $P = 0.04$). The Tumor Immune Estimation Resource discovered a link between ALG3 expression and tumor-infiltrating immune cells in LUAD. Additionally, ROC analysis proved that ALG3 is a reliable diagnostic marker for LUAD ($AUC:0.923$). Functional pathways analysis identified that ALG3 is negatively correlated with FAT4. We performed qRT-PCR to assess that knockdown ALG3 expression significantly upregulated FAT4 expression. Spheroid assay and flow cytometry analysis results showed that downregulated of ALG3 inhibited H1975 cell line stemness. Western blot analysis revealed that decreased ALG3 inhibited the YAP/TAZ signal pathway.

Conclusion: High expression of ALG3 is strongly associated with poor prognosis and immune infiltrates in LUAD.

1. Introduction

Lung cancer is one of the most common cancers and the leading cause of cancer-related deaths [1]. On the other hand, adenocarcinoma is the most prevalent pathological type of lung cancer that constitutes nearly 40% of all lung malignancy cases [2]. Molecular detection has greatly improved the precision of cancer treatment and targeted therapies have remarkably enhanced the survival rate of patients with driver genes [3]. Nonetheless, the 5-year survival rate for those with lung adenocarcinoma (LUAD) is less than 15%. As a result, finding novel tumor biomarkers and other possible genetic targets is critical.

Glycosylation plays a crucial role in various cellular processes, including cellular recognition, signaling, and interactions with the extracellular matrix [4]. Minor modifications in glycan structures can have significant effects on cell biology and can also impact the effectiveness of treatments [5,6], making targeting glycosylation an intriguing avenue for cancer drug development [7]. Deregulated expression of high-mannose type N-glycans has been shown to be associated with the progression of cancer [8]. Alpha-1, 3-mannosyltransferase (ALG3) is an ALG family member discovered on chromosome 3q27.1 [9]. ALG3 expression was shown to be overexpressed in multi-drug resistance cells [10], ALG3 overexpression results in glycoprotein malfunction, which promotes tumor cell proliferation and invasion. However, the clinical significance functional role of ALG3 in LUAD has not yet understood.

The aim of this study was to utilize comprehensive bioinformatics analysis to explore the prognostic significance of AL3 in lung adenocarcinoma. To assess the association between immune cell infiltration and ALG3 expression, we employed the Tumor Immune Estimate Resource (TIMER) and conducted Gene Set Enrichment Analysis (GSEA). Additionally, we observed that knocking down ALG3 expression suppressed the proliferation of H1975 stem cell through modulation of the YAP/TAZ pathway. Our findings highlight the potential of ALG3 as a diagnostic and prognostic marker for LUAD.

2. Materials and methods

2.1. Cell culture

The lung cancer cell lines H1975 and A549 were purchased from Procell. The cells are cultured in RPMI1640 (Gibco) supplemented with 10% FBS (Gibco) under conditions of 5% CO₂ and 37 °C. siRNA negative control and siALG3 were chemically synthesized by RiboBio (Guangzhou, China). We transfected the siRNA negative and siALG3 following Lipofectamine 3000 (Invitrogen). After a transfection period of 48 h, cells were collected for subsequent experiments.

2.2. Database search

TCGA and Genotype Tissue Expression (GTEx) databases were searched to retrieve information related to transcriptional levels and relevant clinical data of 33 cancer types by UCSC XENA [11]. The RNA-Seq transcriptome data was transformed into TPM format and Log₂ for further analysis. Ethics approval was not required for this study. The Wilcoxon rank-sum test was used to examine the data. $P < 0.05$ was significant.

The expression data of ALG3 in lung adenocarcinoma was collected from the TCGA database. A comprehensive analysis was conducted using a total of 535 lung adenocarcinoma samples and 59 adjacent normal tissue samples. The ALG3 gene expression data was integrated with essential clinical information, including age, gender, smoker condition, T stage, N stage, M stage, and tumor location.

2.3. Gene interaction networks

GEPIA is a user-friendly web server that facilitates the analysis of RNA sequencing data from both the TCGA and Genotype-Tissue Expression (GTEx) projects (<http://gepia.cancer-pku.cn/>). It provides an interactive platform for researchers to explore and interpret gene expression patterns in various tissues and cancer types. In GEPIA, 9736 cancer samples along with 8587 normal samples were analyzed under the TCGA as well as GTEx projects. ALG3 plotting was performed on the X-axis, and the correlation with co-expressed genes was plotted using the Spearman method on the Y-axis [12].

2.4. Kaplan–Meier (KM) plotter data

In this study, we investigated the association between ALG3 expression and key clinical outcomes, including overall survival (OS), disease-free survival (DFS) and progression-free interval, in patients with lung adenocarcinoma. LUAD samples were classified into two categories with the aid of median expression (high versus low expression) and analyzed by the KM plotter (<https://www.xiantaozi.com/>) [13]. The median levels of mRNA, as well as hazard ratio (HR), 95% confidence interval (CI), and P values. HR with 95% CI and P values were computed by the log-rank test in KM Plotter. $P < 0.05$ was significant.

2.5. The Human Protein Atlas (HPA)

The Human Protein Atlas is a valuable and extensive database that offers a comprehensive mapping of human proteins in various cells, tissues, and organs. This mapping is accomplished by integrating diverse omics technologies, including antibody-based imaging [14]. In our study, we performed a comparative analysis to assess the protein expression of ALG3 in both normal and LUAD tissues.

2.6. TIMER database

TIMER is a valuable online tool that offers a comprehensive resource for studying immune infiltration in different types of cancer. In our study, we utilized TIMER to investigate the correlation between ALG3 expression and immune infiltrates in lung adenocarcinoma [15].

2.7. ROC and nomogram analysis

Univariate Cox proportional hazards regression analysis was utilized to examine the relationship between gene expression and overall survival in patients. Subsequently, the least absolute shrinkage and selection operator (LASSO)-Cox method was employed to construct a prognostic risk score model. By utilizing the median risk score of the training dataset, each patient was classified into either a low or a high-risk group. Low-risk patients exhibited higher overall survival rates, whereas high-risk patients had lower overall survival rates. To evaluate the sensitivity and specificity of diagnostic and prognostic prediction models, a receiver operating characteristic (ROC) curve was employed. Nomograms were developed using R software version 3.5.1 for establishing the prognostic risk score model.

2.8. Western blot

Western blot analysis was conducted to determine the expression of ALG3, FAT4, YAP, TAZ, GAPDH and phosphorylation YAP. Antibodies against ALG3 (Proteintech#20290-1-AP, 1:1500), FAT4 (SAB#37293, 1:1000), YAP (Proteintech#66900,1:8000), TAZ (Proteintech#23306,1:5000), GAPDH (Proteintech#60004, 1:20000), phosphor-YAP1 (SAB#13401, 1:1500). Each protein expression was detected using Super ECL Plus Detection Reagent (Thermo)

2.9. Quantitative real-time PCR

Cells were treated with Trizol Reagent (Invitrogen) to extract total RNA, following the provided instructions. The concentration of the RNA was determined using a NanoDrop (KAIAO) spectrophotometer. Subsequently, reverse transcription was performed using the Prime Script RT Master Mix reagent (Takara) to synthesize complementary DNA (cDNA). Quantitative real-time PCR was carried out using SYBR Green PCR master mix (Roche). The fold change in the gene expression was calculated with the $2^{-\Delta\Delta Ct}$ method, with GAPDH serving as the internal reference.

2.10. Spheroid assay

The cells were cultured in serum-free DMEM medium supplemented with 20 ng/ml epidermal growth factor, 20 ng/ml basic fibroblast growth factor and B27. Subsequently, the cells were seeded onto an ultra-low-attachment plate at a density of 7.0×10^5 . The formation of spheroids was captured using a microscope (Olympus).

2.11. Flow cytometry

H1975 cells were seeded in 6-well plates at an appropriate concentration and cultured for 48 h. Afterward, the cells were harvested, filtrated and centrifuged. PE-labeled anti-CD44 antibody was employed for staining. The CD44⁺ cells were then incubated with fluorescence-conjugated monoclonal antibodies and detected using flow cytometry (Invitrogen) by quantitation the fluorescence intensity.

2.12. Statistical analysis

Significant quantitative differences between and among groups were assessed using a two-tail *t*-test and one-way ANOVA. Kaplan-

Meier analysis was conducted to compare the overall survival (OS) rate based on the ALG3 expression, with the p-value determined using a log-rank test. The diagnostic value of ALG3 gene expression was evaluated using a receiver operating characteristic (ROC) curve. Univariate Cox analysis was performed to examine potential prognostic factors, while multivariate Cox analysis was utilized to confirm the impact of ALG3 expression on survival. A nomogram was employed to predict overall survival in LUAD patients, incorporating the expression value of ALG3. The expression level of ALG3 in LUAD and normal individuals was further validated using the TIMER database (<https://cistrome.shinyapps.io/timer/>). A p-value of less than 0.05 was considered statistically significant.

3. Results

3.1. High ALG3 expression in LUAD

To examine ALG3 expression in LUAD patients, 594 patients with clinical characteristics were screened from the TCGA data portal (Table 1). ALG3 expression was associated with N stage ($P = 0.009$), pack year ($P = 0.040$), smoking status ($P = 0.028$), and OS ($P < 0.001$), but not with other clinical characteristics. When we compared ALG3 mRNA levels in 535 LUAD and 59 normal tissue samples, we found that ALG3 mRNA levels were higher in LUAD tissues (Fig. 1A and Supplementary Fig. 1A, $P < 0.001$). A matched data analysis indicated that the ALG3 mRNA levels in LUAD ($n = 57$) were significantly higher than in adjacent normal tissues (Fig. 1B, $n = 57$; 5.634 ± 0.511 vs. 4.565 ± 0.28 , $P < 0.001$). To validate the findings, we matched ALG3 protein expression on UALCAN CPTAC database. Patients with LUAD exhibited significantly higher ALG3 expression than normal tissues ($P < 0.05$; Fig. 1C). Similarly, immunohistochemical staining of HPA tissues revealed that ALG3 expression increased in LUAD tissues (Fig. 1D). According to the Kaplan–Meier survival analysis, increased ALG3 expression was associated with poor OS ($P < 0.001$), DSS ($P < 0.001$), and progression-free interval ($P = 0.007$) (Fig. 1E). Collectively, the results suggest that ALG3 overexpression may play a crucial role in LUAD.

3.2. The diagnostic value of ALG3 expression in LUAD

Logistic regression analysis was conducted to investigate the association between ALG3 expression and the clinical characteristics in patients with LUAD (Table 2 and Fig. 2A–D). ALG3 expression was strongly associated with smoking history (Yes vs. No: OR = 1.799, 95% CI = 1.096–2.994, $P = 0.022$), number of pack years (≥ 40 vs. ≤ 40 : OR = 1.572, 95% CI = 1.043–2.378, $P = 0.031$), TNM stage (N0 vs. N2, N3, and N4, OR = 1.759, 95% CI = 1.216–2.558, $P = 0.003$), and pathological stage of patients (stages I, II, III and IV, OR = 1.567, 95% CI = 1.026–2.410, $P = 0.039$). Other clinical pathological features, such as T stage ($P = 0.070$), M stage ($P = 0.280$), gender ($P = 0.361$), and age ($P = 0.331$), on the other hand, did not correlate with ALG3 expression.

ALG3 expression was found to be negatively correlated with OS for patients with N stage (N0, HR = 1.98, $P = 0.002$), pathological stage (stage I, HR = 2.09, $P = 0.003$), and number of pack years (< 40 , HR = 2.58, $P = 0.001$; Fig. 2E–G). Elevated ALG3 expression emerged as an independent prognostic factor significantly impacting overall survival, ALG3 was shown to be positively related to N

Table 1
Clinical characteristics of the lung adenocarcinoma patients (TCGA).

Characteristic	Low expression of ALG3	High expression of ALG3	p
n	267	268	
T stage, n (%)			0.322
T1	97 (18.2%)	78 (14.7%)	
T2	137 (25.8%)	152 (28.6%)	
T3	23 (4.3%)	26 (4.9%)	
T4	8 (1.5%)	11 (2.1%)	
N stage, n (%)			0.009
N0	187 (36%)	161 (31%)	
N1	41 (7.9%)	54 (10.4%)	
N2	26 (5%)	48 (9.2%)	
N3	1 (0.2%)	1 (0.2%)	
Gender, n (%)			0.409
Female	148 (27.7%)	138 (25.8%)	
Male	119 (22.2%)	130 (24.3%)	
Age, n (%)			0.376
≤ 65	120 (23.3%)	135 (26.2%)	
> 65	134 (26%)	127 (24.6%)	
number_pack_years smoked, n (%)			0.040
< 40	99 (26.8%)	89 (24.1%)	
≥ 40	75 (20.3%)	106 (28.7%)	
Smoker, n (%)			0.028
No	46 (8.8%)	29 (5.6%)	
Yes	209 (40.1%)	237 (45.5%)	
OS event, n (%)			<0.001
Alive	191 (35.7%)	152 (28.4%)	
Dead	76 (14.2%)	116 (21.7%)	

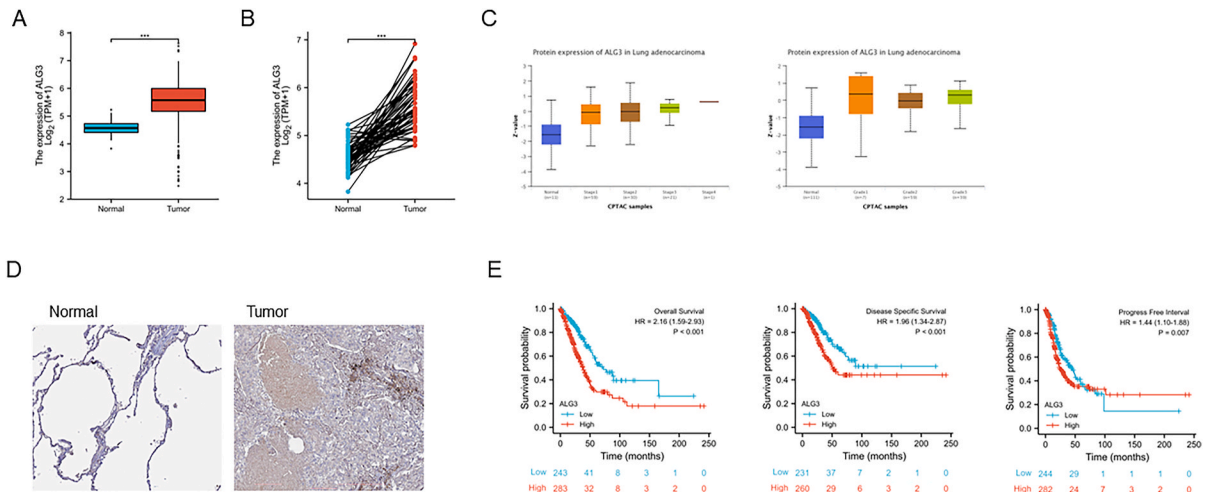


Fig. 1. The expression level of ALG3 in lung adenocarcinoma. (A) The mRNA expression of ALG3 in average ($n = 59$) and tumor tissues ($n = 535$). (B) The expression of ALG3 in 57 paired lung cancer tissues. (C) The protein expression of ALG3 based on CPTA in patients with lung adenocarcinoma according to different clinical characteristics. (D) LUAD tissue immunohistochemically stained for ALG3. (E) Kaplan-Meier survival curve based on ALG3 expression levels in patients with lung adenocarcinoma is correlated with overall survival, disease-specific survival, and progress free internal.

Table 2
Logistic analysis of the correlation between ALG3 expression and clinical features.

Characteristics	Total(N)	Odds Ratio (OR)	P value
T stage (T2&T3&T4 vs. T1)	532	1.399 (0.974–2.015)	0.070
N stage (N1&N2&N3 vs. N0)	519	1.759 (1.216–2.558)	0.003
M stage (M1 vs. M0)	386	1.577 (0.697–3.714)	0.280
Pathologic stage (Stage III&Stage IV vs. Stage I&Stage II)	527	1.567 (1.026–2.410)	0.039
Gender (Male vs. Female)	535	1.172 (0.834–1.647)	0.361
Age (>65 vs. ≤ 65)	516	0.842 (0.596–1.190)	0.331
Smoker (Yes vs. No)	521	1.799 (1.096–2.994)	0.022
number_pack_years_smoked (≥ 40 vs. <40)	369	1.572 (1.043–2.378)	0.031

Stage (HR = 2.069, $P < 0.001$), T Stage (HR = 2.464, $P < 0.001$), and residual tumor (HR = 2.199, $P < 0.014$; Fig. 3A) in multivariate Cox regression analysis. High ALG3 expression was an independent factor affecting overall survival (HR = 1.325, $P = 0.04$). In addition, a nomogram was constructed to predict T stage, N stage, and residual tumor, as well as ALG3 expression at 1-, 3-, and 5-year OS in patients with LUAD (Fig. 3B). The calibration plots of the nomogram provided a prediction for the results after 1, 3, and 5 years (Fig. 3C). Furthermore, we conducted a comparison between normal lung tissue and LUAD tissue to generate a receiver operating characteristic (ROC) curve and evaluate the diagnostic efficacy of ALG3. The area under the curve in LUAD was 0.923, indicating that ALG3 exhibits a high diagnostic value (Fig. 3D). Therefore, ALG3 may serve as a useful prognostic indicator of survival in patients with LUAD.

3.3. Analysis of functional pathways associated with ALG3 expression in LUAD

We examined 13,787 genes co-expressed with ALG3 in the TCGA database to learn more about its possible role in LUAD. The outcome displays the top 50 genes that are both positively and negatively associated with the ALG3 gene (Fig. 4A and Supplementary Figs. 2A–B). *NOC4L* ($r = 0.698$, $P < 0.001$), *ABCF3* ($r = 0.778$, $P < 0.001$), and *ECE2* ($r = 0.760$, $P < 0.001$) were the top three positively linked genes, whereas *CREBRF* ($r = -0.495$, $P < 0.001$), *DMXLI* ($r = -0.479$, $P < 0.001$), and *FAT4* ($r = -0.506$, $P < 0.001$) were the top three adversely related genes. The DAVID database indicated that the genes were shown to be positively related to oxidative phosphorylation, reactive oxygen species, metabolic pathways, DNA replication, and cell cycle (Fig. 4B). In addition, we used GSEA to identify metabolic pathways (Fig. 5A). GPCR ligand binding, rhodopsin-like GPCRs, and RHO GRPase signaling pathways were strongly correlated with ALG3 expression (Fig. 5B–C).

3.4. ALG3 promoted H1975 stem cell proliferation

We measured ALG3 and FAT4 expression levels in A549 and H1975 cells and found that ALG3 was elevated whereas FAT4 was down regulated. (Fig. 6A–B), this consistent with the co-expression analysis of ALG3. As FAT4 was reported to be a tumor suppressor

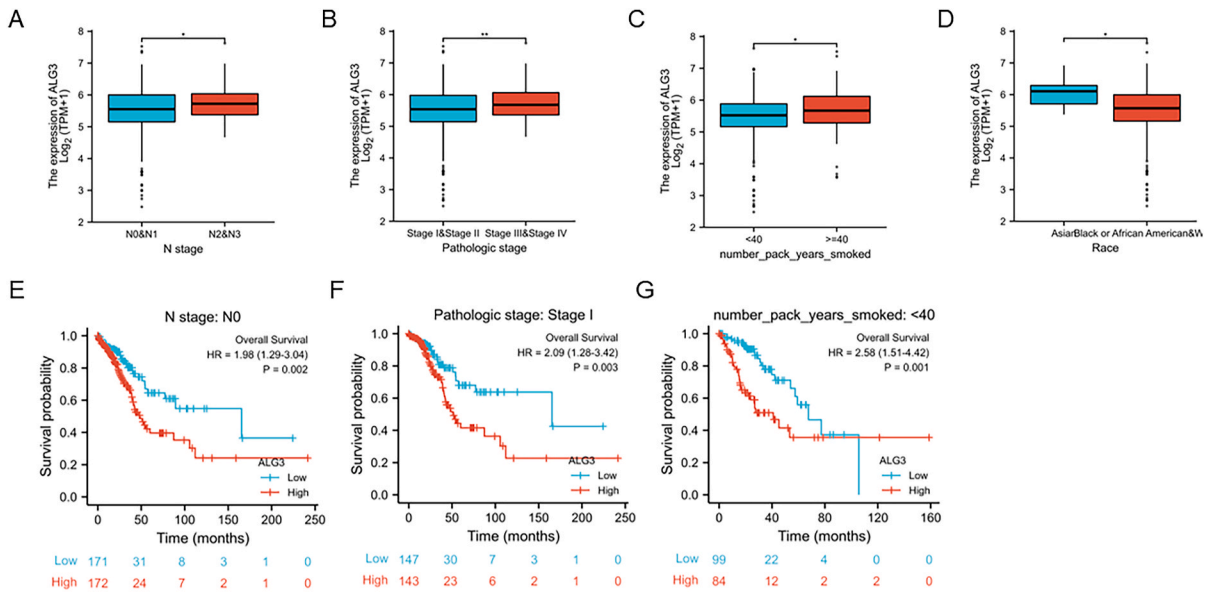


Fig. 2. ALG3 expression correlates with different clinical characteristics. The relationship between ALG3 expression and clinical features, including (A) smoking history, (B) number of pack years, (C) TNM stage, and (D) pathological stage of patients. Kaplan-Meier survival curve of different clinical subgroups, including (E) N. stage N0. (F) Pathologic stage I. (G) Number pack years smoked.

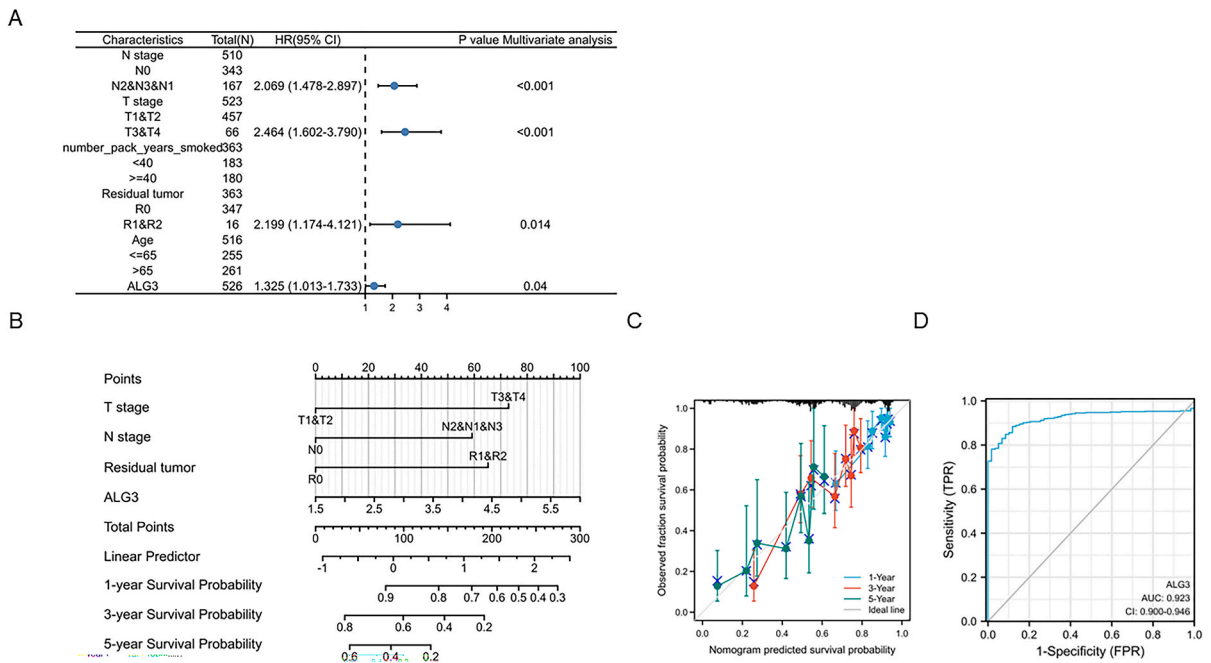


Fig. 3. The prognosis value of ALG3 in lung adenocarcinoma. (A) Forest plot of lung adenocarcinoma patients based on multivariate Cox regression analysis. (B) A nomogram for predicting the probability that patients with 1, 3, and 5 years of overall survival. (C) Calibration plots of the nomogram provided predictions for 1, 3, and 5 years. (D) The ROC curves of ALG3 in patients with LUAD and standard control.

that regulated Hippo/YAP pathway in mammalian tissue development, differentiation and tumorigenesis [16]. To investigate the potential involvement of ALG3 in tumor initiation through the YAP signaling pathway, we employed siRNA targeting ALG3 and non-silencing RNA sequences for transfected into the H1975 cell line. The efficiency of knockdown was validated through qRT-PCR analysis, as shown in Fig. 6C. The result revealed a significant decrease in ALG3 expression following siALG3 transfection. To explore the role of ALG3 in stem cell initiation, the spheroid assay was performed. Notably, the inhibition of ALG3 resulted in a marked reduction in stem cell formation, as shown in Fig. 6D. Additionally, flow cytometry analysis using CD44, a marker of tumor aggression,

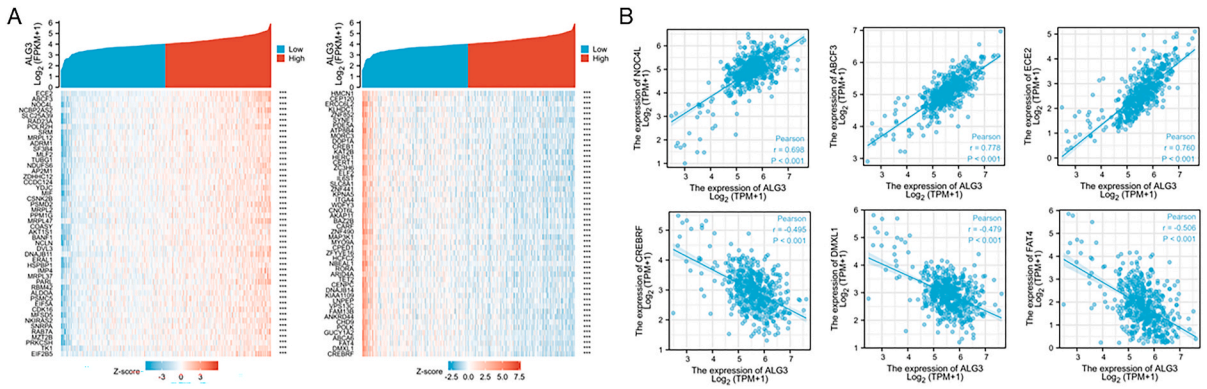


Fig. 4. ALG3 co-expression genes in LUAD analyzed by String database. (A) The gene co-expression heatmap of the top 50 positively and negatively correlated with ALG3 in the LUAD cohort. (B) The correlation analyses between the expression of ALG3 and positively correlated genes (NOCAL, ABCF3, and ECE2), and negative correlated genes (CREBRF, DMXL1, and FAT4).

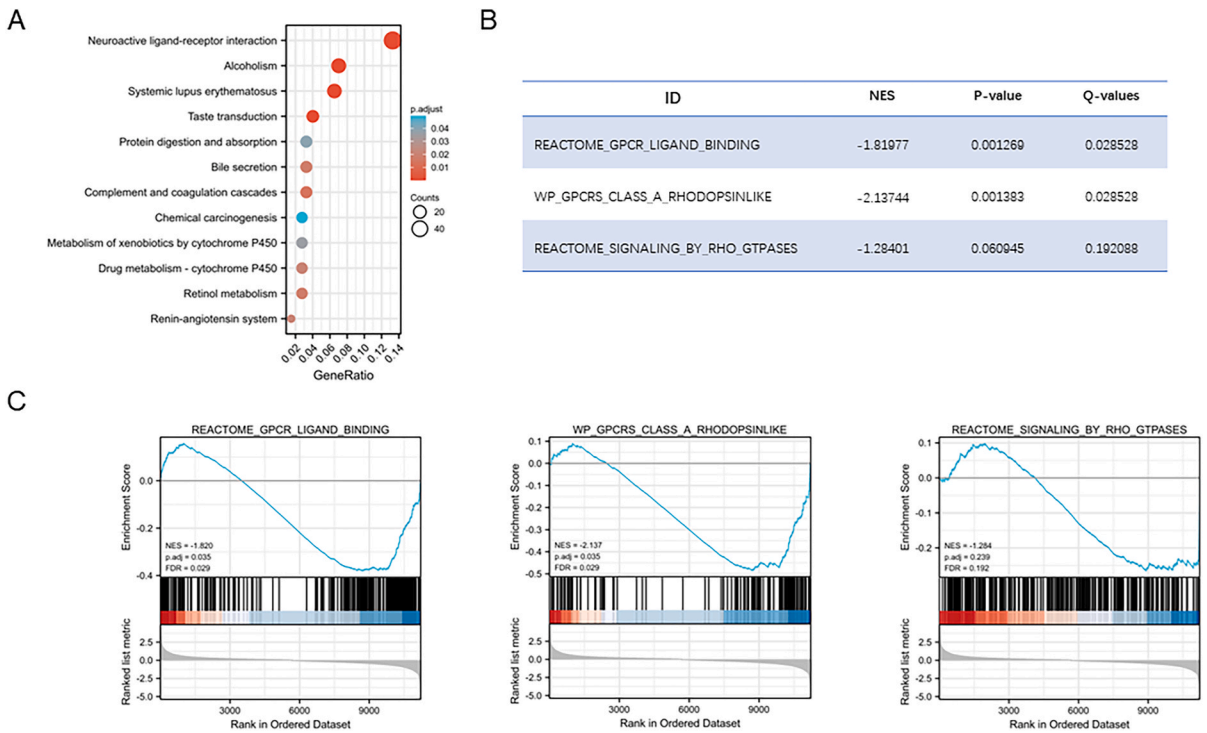


Fig. 5. Functional enrichment analysis of ALG3 in lung adenocarcinoma. (A) Functional enrichment analysis of involved genes. (B) Gene sets associated with high ALG3 expression. (C) Enrichment plots of ALG3 relevant enrichment pathways in GSEA analysis.

was conducted to further elucidate the role of ALG3 in tumor initiation. The results demonstrated a decrease in CD44 positive lung cancer cells following ALG3 knockdown (Fig. 6E). To verify the underlying mechanism, we assessed the protein expression of the YAP signaling pathway by Western blot. As a result of ALG3 knockdown, FAT4 expression increased along with decreased YAP, TAZ and YAP phosphorylation (Fig. 6F). These results showed a good consistency with predictive model.

3.5. Link between ALG3 expression and immune cell infiltration in LUAD

We utilized the TIMER database to explore the potential correlation between ALG3 expression and immune cell infiltration (Fig. 7A). ALG3 expression was associated with type 2 T cells ($r = 0.236, P < 0.001$), CD56, dim natural killer cells ($r = 0.198, P < 0.001$), and gamma-delta T cells ($r = 0.151, P < 0.001$). ALG3 expression was inversely correlated with CD 8 T cells ($r = 0.143, P < 0.001$), Mast cells ($r = -0.167, P < 0.001$), Eosinophils ($r = -0.112, P = 0.010$), Macrophages ($r = -0.149, P < 0.001$), Effective memory T-cells ($r = -0.283, P < 0.001$) and central memory T-cells ($r = -0.477, P < 0.001$) (Fig. 7B). ADCs, cytotoxic cells, CD56

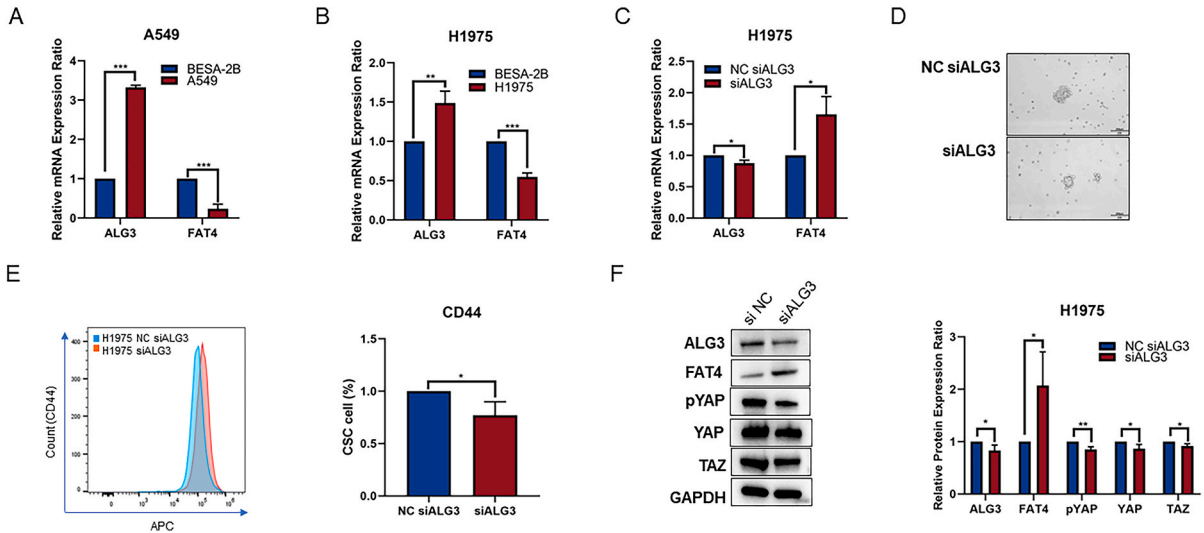


Fig. 6. ALG3 promoted H1975 stem cell proliferation. (A) qPCR analysis showed mRNA expression of ALG3 and FAT4 in A549 cell. (B) qPCR analysis showed mRNA expression of ALG3 and FAT4 in H1975 cell. (C) qPCR analysis showed mRNA expression ALG3 and FAT4 in H1975 cell transfected with siALG3. (D) Representative pictures of H1975 spheroids transfected with siALG3. (E) Flow cytometry analysis of CD44 expression in H1975 cell transfected with siALG3. (F) Western blot analysis ALG3, FAT4, YAP, TAZ, and YAP phosphorylation expression of H1975 siALG3 cells. * $P < 0.05$, ** $P < 0.01$.

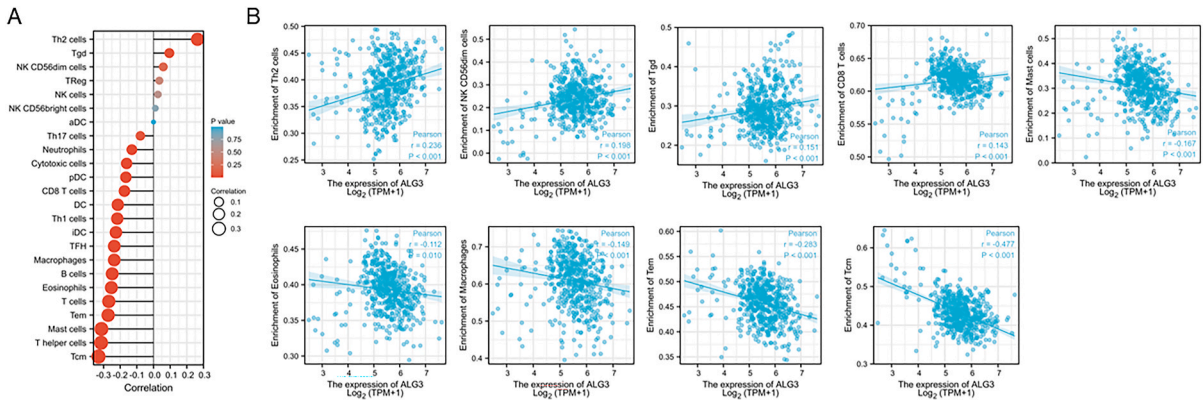


Fig. 7. Correlation of ALG3 expression with immune infiltration level. (A) ALG3 expression is correlated with Th2 cells, NK DC56dim cells, gamma delta T cells, CD8 T cells, mast cells, eosinophils, effective memory T cells, macrophages, central memory T cells, and DC cells. (B) The relationship between ALG3 expression and immune subtypes in lung adenocarcinoma.

bright NK cells, NK cells, T-helper cells 17, and regulatory T-cells, on the other hand, did not show any significant relationship with ALG3 expression.

4. Discussion

The glycosylation of N-linked proteins plays a crucial role in multiple of cancer processes, including cell survival, proliferation, migration, metastasis, and anti-tumor immunity [17–19]. Therefore, abnormalities expression of glycosyltransferase is considered to be predictive markers and therapeutic targets in tumors [20]. We used the Kaplan–Meier plot to determine the prognostic value of the ALG3. Individuals with high levels of ALG3 mRNA exhibited worse OS, DSS, DFS. According to multivariate Cox analysis, elevated ALG3 expression emerged as an independent predictor of poor outcomes in LUAD.

The ALG3 gene produces an alpha-1, 3-mannosyltransferase that helps to produce glycans in the endoplasmic reticulum and Golgi complex. ALG3 expression is significantly increased in OSCC tissues and is associated with pathological stage lymph node metastasis [21]. The increased expression of ALG3 is thought to activate the CDK-cyclin pathway [22]. Moreover, ALG3 overexpression in breast cancer patients predicts poor clinical features, OS, and early local recurrence-free survival [23,24]. ALG3 promotes radiation resistance and cancer stemness by glycosylating TGF- β receptor II [25]. Therefore, radiation is crucial in preventing early recurrence of

breast cancers in women with low ALG3 levels. Using N-glycans profiles of membrane proteins, Liu reported that adriamycin-resistant cells exhibited strong binding of membrane proteins with MAM-M and ConA lectins, which are specific for mannose. Detection of ALG3 enzyme levels revealed that high levels of mannose N-glycan corresponded to acute myeloid leukemia cell-related drug resistance. Consistent with these findings, we observed that ALG3 expression was remarkably increased in LUAD, and ALG3 positively co-expressed with ATP-binding cassette transporter member *ABCF3*. The ABC gene expression profiles were associated with stem cell pluripotency and pathological response to chemotherapy. Bioinformatic analyses indicated that *ABCF3* downregulation was associated with the chemotherapy sensitivity and progression of the disease [26]. Furthermore, we discovered that ALG3 was negatively co-expressed with FAT4. FAT4 has been identified as a tumor suppressor in non-small lung cancer [27]. FAT4 suppression has been seen as an important factor in cancer progression and chemosensitivity via regulating the HIPPO signaling pathway, which controls cell proliferation, stem cell renewal, and differentiation [28,29].

Extensive evidence has demonstrated the association between cancer stem-like traits and cancer progression, which contributes to early cancer relapse. Post-transcriptional modifications, particularly glycosylation, have been reported to play a significant role in the acquisition of cancer stem-like traits in various types of cancers [30,31]. We hypothesized that increased ALG3 expression promote stemness in LUAD. In this study, we found that ALG3 knockdown significantly inhibited sphere formation ability and decreased the proportion of CD44 cells. However, additional research is needed to corroborate this.

The presence of mannose glycans has been identified as a prognostic indicator associated with unfavorable outcomes. In esophageal squamous cell carcinoma, ALG3 amplification has been linked to lymph node metastasis, highlighting its potential as a therapeutic target. Additionally, our findings several a significant correlation between increased ALG3 levels and adverse clinical outcomes, including T staging, lymph node metastasis, and tissue differentiation, further emphasizing the importance of AGL3 as a prognostic marker in this context. ALG3 expression is positively related to the progression of NSCLC, implying a role of ALG3 in carcinogenesis. ALG3 knockdown inhibited NSCLC cells growth and migration. ALG3 and CD8⁺ T cells infiltration have been linked to advanced tumor stage. C-type lectins bind to glycans, triggering immunostimulatory or immunosuppressive pathways through the immune system [32, 33]. N-glycosylation removal would reveal related immunogenic epitopes, enhance immune recognition and improve immunosurveillance in cancer [34]. Macrophages, T cells, as well as B cells, infiltrate the tumor microenvironment in lung cancer. The expression of ALG3 in immune cells was examined in this study. The antitumor effects of ALG3 in lung cancer are mediated by B cells, CD4⁺ T cells [35,36]. ROC analysis indicated that ALG3 expression had some diagnostic value at various stages of LUAD. Based on survival analyses, ALG3 expression was associated with worse survival outcomes among LUAD patients. Furthermore, ALG3 expression was linked to the infiltration of various immune cells that play an important role in tumorigenesis. Collectively, these results suggested that ALG3 is a potential viable biomarker for prognosis anticipation and diagnosis of LUAD patients.

5. Conclusions

In conclusion, we extensively examined the expression pattern as well as prognostic value of ALG3 in patients with LUAD using bioinformatic analyses. Our results suggested that ALG3 overexpression is linked to immune infiltration as well as poorer prognosis. Thus, ALG3 can be used as an independent prognostic factor for predicting OS among LUAD patients.

Author contribution statement

Linxuan Huang, Ruinian Zheng: Conceived and designed the experiments; BaoCheng Xie, Caixiang Liu, Zhiming Wu: Performed the experiments; Dongbo Guo, Guanming Jiang, Guowei Lai Analyzed and interpreted the data; Yinjiao Yuan, Yu Zhang, Xiarong Hu Contributed reagents, materials, analysis tools or data; Linxuan Huang, Yinjiao Yuan, Yu Zhang, Wrote the paper.

Funding

This study was supported in part by a grant from the Guangdong Basic and Applied Basic Research Foundation, China (No. 2021B1515140031 and 2020A1515110029), Dongguan Science and Technology of Social Development Program, China (No. 2019507163147, 20211800905222 and 2020507163160), Postdoctoral Foundation of Dongguan People's Hospital, China (No. K202009), Natural Science Foundation of Guangdong Province natural science fund of Guangdong, China (No. 2021A1515010156 and 2022A1515140134) and National Natural Science Foundation of China (No. 32100627).

Availability of data and materials

The datasets supporting the conclusions of this article are included within the article.

Declaration of competing interest

The authors declare that they have no known competing financial interests or personal relationships that could have appeared to influence the work reported in this paper.

Acknowledgements

Not applicable.

Appendix A. Supplementary data

Supplementary data to this article can be found online at <https://doi.org/10.1016/j.heliyon.2023.e18065>.

References

- [1] R.L. Siegel, K.D. Miller, H.E. Fuchs, A. Jemal, Cancer statistics, 2022, *Ca-Cancer, J. Clin.* 72 (1) (2022) 7–33, <https://doi.org/10.3322/caac.21708>.
- [2] A. Friedlaender, G. Banna, U. Malapelle, P. Pisapia, A. Addeo, Next generation sequencing and genetic alterations in squamous cell lung carcinoma: where are we today? *Front. Oncol.* 9 (2019) 166, <https://doi.org/10.3389/fonc.2019.00166>.
- [3] P. Nanavaty, M.S. Alvarez, W.M. Alberts, Lung cancer screening: advantages, controversies, and applications, *Cancer Control* 21 (1) (2014) 9–14, <https://doi.org/10.1177/107327481402100102>.
- [4] A. Varki, Biological roles of glycans, *Glycobiology* 27 (1) (2017) 3–49, <https://doi.org/10.1093/glycob/cww086>.
- [5] V. Barbier, J. Erhani, C. Fiveash, J.M. Davies, J. Tay, M.R. Tallack, J. Lowe, J.L. Magnani, D.R. Pattabiraman, A.C. Perkins, J. Lisle, J. Rasko, J.P. Levesque, I. G. Winkler, Endothelial e-selectin inhibition improves acute myeloid leukaemia therapy by disrupting vascular niche-mediated chemoresistance, *Nat. Commun.* 11 (1) (2020) 2042, <https://doi.org/10.1038/s41467-020-15817-5>.
- [6] L. Shen, M. Xia, X. Deng, Q. Ke, C. Zhang, F. Peng, X. Dong, Z. Luo, A lectin-based glycomic approach identifies fut8 as a driver of radioresistance in oesophageal squamous cell carcinoma, *Cell. Oncol.* 43 (4) (2020) 695–707, <https://doi.org/10.1007/s13402-020-00517-5>.
- [7] A.F. Costa, D. Campos, C.A. Reis, C. Gomes, Targeting glycosylation: a new road for cancer drug discovery, *Trends Cancer* 6 (9) (2020) 757–766, <https://doi.org/10.1016/j.trecan.2020.04.002>.
- [8] J. Munkley, I.G. Mills, D.J. Elliott, The role of glycans in the development and progression of prostate cancer, *Nat. Rev. Urol.* 13 (6) (2016) 324–333, <https://doi.org/10.1038/nrurol.2016.65>.
- [9] F. Trempel, H. Kajiura, S. Ranf, J. Grimmer, L. Westphal, C. Zipfel, D. Scheel, K. Fujiyama, J. Lee, Altered glycosylation of exported proteins, including surface immune receptors, compromises calcium and downstream signaling responses to microbe-associated molecular patterns in arabidopsis thaliana, *BMC Plant Biol.* 16 (2016) 31, <https://doi.org/10.1186/s12870-016-0718-3>.
- [10] B. Liu, X. Ma, Q. Liu, Y. Xiao, S. Pan, L. Jia, Aberrant mannosylation profile and ftx/mir-342/alg3-axis contribute to development of drug resistance in acute myeloid leukemia, *Cell Death Dis.* 9 (6) (2018) 688, <https://doi.org/10.1038/s41419-018-0706-7>.
- [11] K. Tomczak, P. Czerwinska, M. Wiznerowicz, The cancer genome atlas (tcga): an immeasurable source of knowledge, *Wspólczesna Onkol.* 19 (1A) (2015) A68–A77, <https://doi.org/10.5114/wo.2014.47136>.
- [12] Z. Tang, C. Li, B. Kang, G. Gao, C. Li, Z. Zhang, Gepia: a web server for cancer and normal gene expression profiling and interactive analyses, *Nucleic Acids Res.* 45 (W1) (2017) W98–W102, <https://doi.org/10.1093/nar/gkx247>.
- [13] C.C. Sun, S.J. Li, W. Hu, J. Zhang, Q. Zhou, C. Liu, L.L. Li, Y.Y. Songyang, F. Zhang, Z.L. Chen, G. Li, Z.Y. Bi, Y.Y. Bi, F.Y. Gong, T. Bo, Z.P. Yuan, W.D. Hu, B. T. Zhan, Q. Zhang, Q.Q. He, D.J. Li, Comprehensive analysis of the expression and prognosis for e2fs in human breast cancer, *Mol. Ther.* 27 (6) (2019) 1153–1165, <https://doi.org/10.1016/j.ymthe.2019.03.019>.
- [14] M. Uhlen, C. Zhang, S. Lee, E. Sjostedt, L. Fagerberg, G. Bidkhorri, R. Benfeitas, M. Arif, Z. Liu, F. Edfors, K. Sanli, K. von Feilitzen, P. Oksvold, E. Lundberg, S. Hober, P. Nilsson, J. Mattsson, J.M. Schwenk, H. Brunnstrom, B. Glimelius, T. Sjoblom, P.H. Edqvist, D. Djureinovic, P. Micke, C. Lindskog, A. Mardinoglu, F. Ponten, A pathology atlas of the human cancer transcriptome, *Science* 357 (6352) (2017), <https://doi.org/10.1126/science.aan2507>.
- [15] T. Li, J. Fu, Z. Zeng, D. Cohen, J. Li, Q. Chen, B. Li, X.S. Liu, Timer2.0 for analysis of tumor-infiltrating immune cells, *Nucleic Acids Res.* 48 (W1) (2020) W509–W514, <https://doi.org/10.1093/nar/gkaa407>.
- [16] Z. Feng, Y. Yin, B. Liu, Y. Zheng, D. Shi, H. Zhang, J. Qin, Prognostic and immunological role of fat family genes in non-small cell lung cancer, *Cancer Control* 29 (2022), 1389472566, <https://doi.org/10.1177/10732748221076682>.
- [17] C. Cheng, P. Ru, F. Geng, J. Liu, J.Y. Yoo, X. Wu, X. Cheng, V. Euthine, P. Hu, J.Y. Guo, E. Lefai, B. Kaur, A. Nohturfft, J. Ma, A. Chakravarti, D. Guo, Glucose-mediated n-glycosylation of scap is essential for srebp-1 activation and tumor growth, *Cancer Cell* 28 (5) (2015) 569–581, <https://doi.org/10.1016/j.ccell.2015.09.021>.
- [18] F. Dall’Olio, N. Malagolini, M. Trinchera, M. Chiricolo, Mechanisms of cancer-associated glycosylation changes, *Front. Biosci.* 17 (2) (2012) 670–699, <https://doi.org/10.2741/3951>.
- [19] S.S. Pinho, C.A. Reis, Glycosylation in cancer: mechanisms and clinical implications, *Nat. Rev. Cancer* 15 (9) (2015) 540–555, <https://doi.org/10.1038/nrc3982>.
- [20] C. Zhao, K. Xiong, F. Zhao, A. Adam, X. Li, Glycosylation-related genes predict the prognosis and immune fraction of ovarian cancer patients based on weighted gene coexpression network analysis (wgcn) and machine learning, *Oxidative Med. Cell. Longev.* 2022 (2022), 3665617, <https://doi.org/10.1155/2022/3665617>.
- [21] P. Shao, C. Wei, Y. Wang, Alg3 contributes to the malignant properties of oscc cells by regulating cdk-cyclin pathway, *Oral Dis.* 27 (6) (2021) 1426–1434, <https://doi.org/10.1111/odi.13687>.
- [22] P. Shao, C. Wei, Y. Wang, Alg3 contributes to the malignant properties of oscc cells by regulating cdk-cyclin pathway, *Oral Dis.* 27 (6) (2021) 1426–1434, <https://doi.org/10.1111/odi.13687>.
- [23] M.L. de Leoz, L.J. Young, H.J. An, S.R. Kronewitter, J. Kim, S. Miyamoto, A.D. Borowsky, H.K. Chew, C.B. Lebrilla, High-mannose glycans are elevated during breast cancer progression, *Mol. Cell. Proteomics* 10 (1) (2011) M110–M2717, <https://doi.org/10.1074/mcp.M110.002717>.
- [24] Y. Yang, Y. Zhou, X. Xiong, M. Huang, X. Ying, M. Wang, Alg3 is activated by heat shock factor 2 and promotes breast cancer growth, *Med. Sci. Mon. Int. Med. J. Exp. Clin. Res.* 24 (2018) 3479–3487, <https://doi.org/10.12659/MSM.907461>.
- [25] X. Sun, Z. He, L. Guo, C. Wang, C. Lin, L. Ye, X. Wang, Y. Li, M. Yang, S. Liu, X. Hua, W. Wen, C. Lin, Z. Long, W. Zhang, H. Li, Y. Jian, Z. Zhu, X. Wu, H. Lin, Alg3 contributes to stemness and radioresistance through regulating glycosylation of tgf-beta receptor ii in breast cancer, *J. Exp. Clin. Cancer Res.* 40 (1) (2021) 149, <https://doi.org/10.1186/s13046-021-01932-8>.
- [26] K. Seborova, R. Vaclavikova, P. Soucek, K. Elsenrova, A. Bartakova, P. Cernaj, J. Bouda, L. Rob, M. Hrudka, P. Dvorak, Association of abc gene profiles with time to progression and resistance in ovarian cancer revealed by bioinformatics analyses, *Cancer Med.* 8 (2) (2019) 606–616, <https://doi.org/10.1002/cam4.1964>.
- [27] W. Wang, Q. Huang, Y. Chen, Z. Huang, Y. Huang, Y. Wang, X. Qi, Z. Liu, L. Lu, The novel fat4 activator jujuboside a suppresses nsc tumorigenesis by activating hippo signaling and inhibiting yap nuclear translocation, *Pharmacol. Res.* 170 (2021), 105723, <https://doi.org/10.1016/j.phrs.2021.105723>.
- [28] L. Jia, W. Gu, Y. Zhang, B. Jiang, X. Qiao, Y. Wen, Activated yes-associated protein accelerates cell cycle, inhibits apoptosis, and delays senescence in human periodontal ligament stem cells, *Int. J. Med. Sci.* 15 (11) (2018) 1241–1250, <https://doi.org/10.7150/ijms.25115>.
- [29] B. Yeung, J. Yu, X. Yang, Roles of the hippo pathway in lung development and tumorigenesis, *Int. J. Cancer* 138 (3) (2016) 533–539, <https://doi.org/10.1002/ijc.29457>.

- [30] J. Stadlmann, J. Taubenschmid, D. Wenzel, A. Gattinger, G. Durnberger, F. Dusberger, U. Elling, L. Mach, K. Mechtler, J.M. Penninger, Comparative glycoproteomics of stem cells identifies new players in ricin toxicity, *Nature* 549 (7673) (2017) 538–542, <https://doi.org/10.1038/nature24015>.
- [31] Y.C. Wang, S.E. Peterson, J.F. Loring, Protein post-translational modifications and regulation of pluripotency in human stem cells, *Cell Res.* 24 (2) (2014) 143–160, <https://doi.org/10.1038/cr.2013.151>.
- [32] M.S. Pereira, I. Alves, M. Vicente, A. Campar, M.C. Silva, N.A. Padrao, V. Pinto, A. Fernandes, A.M. Dias, S.S. Pinho, Glycans as key checkpoints of t cell activity and function, *Front. Immunol.* 9 (2018) 2754, <https://doi.org/10.3389/fimmu.2018.02754>.
- [33] Y. van Kooyk, G.A. Rabinovich, Protein-glycan interactions in the control of innate and adaptive immune responses, *Nat. Immunol.* 9 (6) (2008) 593–601, <https://doi.org/10.1038/nif.203>.
- [34] M.C. Silva, A. Fernandes, M. Oliveira, C. Resende, A. Correia, J.C. De-Freitas-Junior, A. Lavelle, J. Andrade-Da-Costa, M. Leander, H. Xavier-Ferreira, J. Bessa, C. Pereira, R.M. Henrique, F. Carneiro, M. Dinis-Ribeiro, R. Marcos-Pinto, M. Lima, B. Lepenies, H. Sokol, J.C. Machado, M. Vilanova, S.S. Pinho, Glycans as immune checkpoints: removal of branched n-glycans enhances immune recognition preventing cancer progression, *Cancer Immunol. Res.* 8 (11) (2020) 1407–1425, <https://doi.org/10.1158/2326-6066.CIR-20-0264>.
- [35] T.C. Bruno, P.J. Ebner, B.L. Moore, O.G. Squalls, K.A. Waugh, E.B. Eruslanov, S. Singhal, J.D. Mitchell, W.A. Franklin, D.T. Merrick, M.D. Mccarter, B.E. Palmer, J.A. Kern, J.E. Slansky, Antigen-presenting intratumoral b cells affect cd4(+) til phenotypes in non-small cell lung cancer patients, *Cancer Immunol. Res.* 5 (10) (2017) 898–907, <https://doi.org/10.1158/2326-6066.CIR-17-0075>.
- [36] N. Inoshima, Y. Nakanishi, T. Minami, M. Izumi, K. Takayama, I. Yoshino, N. Hara, The influence of dendritic cell infiltration and vascular endothelial growth factor expression on the prognosis of non-small cell lung cancer, *Clin. Cancer Res.* 8 (11) (2002) 3480–3486.